# Low temperature selective CO oxidation in excess of $H_2$ over Pt/Ce—$ZrO_2$ catalysts

Hyun-Seog Roh, H.S. Potdar, Ki-Won Jun*, Sang Yun Han, and Jae-Woo Kim

*Chemical Technology Division, Korea Research Institute of Chemical Technology, P.O. Box 107, Yuseong, Daejeon 305-600, Korea*

Received 19 July 2003; accepted 10 January 2004

Pt/Ce—$ZrO_2$ catalysts have been designed and applied to selective CO oxidation at low temperature. Both tetragonal and cubic phase Ce—$ZrO_2$ supports were prepared by co-precipitation method to get high surface area materials after calcination at 500 °C for 6 h in air. Selective CO oxidation was conducted using stoichiometric amounts of $O_2$. Cubic Ce—$ZrO_2$ supported Pt catalyst exhibited 78% CO conversion and 96% $CO_2$ selectivity even at 60 °C, while Pt/$Al_2O_3$ catalyst showed less than 1% CO conversion at the same condition. The higher CO conversion and $CO_2$ selectivity (to $CO_2$ as opposed to $H_2O$) of Pt/Ce—$ZrO_2$ catalyst is mainly due to the high oxygen storage capacity of Ce—$ZrO_2$ and nano-crystalline nature of cubic $Ce_{0.8}Zr_{0.2}O_2$.

**KEY WORDS:** CO oxidation; low temperature; co-precipitation; Pt; Ce—$ZrO_2$.

## 1. Introduction

Proton-exchange membrane (PEM) fuel cells have a series of advantages such as low operating temperature, sustained operation at high current density, low weight, compactness, potential for low cost and volume, long stack life, fast start-ups, suitability to discontinuous operation. Consequently, PEM fuel cells are leading candidates for mobile power applications or for small stationary power units [1–5].

The ideal fuel for PEM fuel cells is pure hydrogen, with less than 50 ppm CO. Low temperature PEM fuel cells utilize the hydrogen produced by an external reformer. The $H_2$-rich reformate typically contains several mol% CO which will poison the anode of PEM fuel cells. Thus, CO should be selectively oxidized while minimizing oxidation of $H_2$. Like other catalytic reactions, the challenges of CO oxidation are activity and selectivity. Since the selective CO oxidation is carried out after the low-temperature shift reactor (~200 °C), it should operate at low temperatures [6].

The low-temperature CO oxidation has been reviewed extensively [7]. However, the number of publications on the selective CO oxidation in $H_2$-rich atmospheres has only increased as a result of the interest in PEM fuel cells [1,6]. Catalysts investigated include Pt [6,8–11], Ru [9], and Au [12]. It was reported that using a low $O_2$ concentration minimizes hydrogen oxidation [8]. Son and Lane [6] reported that CO conversions were improved at low temperatures (100–200 °C) and stoichiometric ratio of $O_2$/CO for Ce-promoted Pt/$\gamma$-$Al_2O_3$.

$CeO_2$ has been considered as the most important rare earth element in catalysis. It plays an important role in three-way catalysis (TWC) and fluid catalytic cracking (FCC) [13,14]. Therefore, much effort has been dedicated to studying the role of ceria. As a result, it is known that the high oxygen storage capacity (OSC) of $CeO_2$ improves catalytic performance by storing oxygen during oxidation and releasing it during reduction [13,14].

Ce-containing mixed oxides have attracted much attention as oxidation catalysts because of their unique redox properties and high OSC [13,14]. It has been reported that the addition of $ZrO_2$ to $CeO_2$ leads to improvements in OSC of $CeO_2$, redox property, thermal resistance and promotion of metal dispersion [14–16], resulting in better performance in CO oxidation [17] and combustion of methane [18]. This was found to be due to the partial substitution of $Ce^{4+}$ with $Zr^{4+}$ in the lattice of $CeO_2$ which results in a solid solution formation [15,17]. Because of better thermal stability as well as their enhanced oxygen mobility, the $Ce_{1-x}$—$Zr_xO_2$ system has appeared as a promising support to be used in catalytic oxidation systems. It has been reported that the cubic phase of Ce—$ZrO_2$ has more OSC and is more easily reducible than the tetragonal phase [17,19,20]. Meeyoo and co-workers [17] reported that cubic $Ce_{1-x}$—$Zr_xO_2$ ($x < 0.5$) showed better CO oxidation performance than tetragonal $Ce_{1-x}$—$Zr_x O_2$ ($x > 0.5$) owing to the advantages of cubic Ce—$ZrO_2$ in the absence of $H_2$. It is also known that Ce—$ZrO_2$ prepared by the co-precipitation method has higher surface area [21].

Based on the above results, we have designed cubic $Ce_{0.8}Zr_{0.2}O_2$ supported Pt catalyst and applied to the selective CO oxidation reaction. In this study, the

---

* To whom correspondence should be addressed.

1011-372X/04/0300–0203/0 © 2004 Plenum Publishing Corporation

selectivity and activity of Pt/Ce—$ZrO_2$ catalysts have been examined in low temperature CO oxidation with stoichiometric amounts of $O_2$.

## 2. Experimental

Tetragonal ($Ce_{0.2}Zr_{0.8}O_2$) and Cubic ($Ce_{0.8}Zr_{0.2}O_2$) supports were prepared by a one-step co-precipitation/digestion method [21]. Stoichiometric quantities of zirconyl nitrate solution (20 wt% in $ZrO_2$ base, MEL Chemicals) and cerrous nitrate (99.9%, Aldrich) were dissolved in distilled water, and the resulting solution was transferred to a round bottom flask. To this above solution an aqueous solution of 20% KOH (w/w) was added drop-wise at 80 °C with constant stirring to attain a pH of 10.5. During the entire course of co-precipitation reactions, the pH was maintained in this alkaline range. The precipitates were digested at 80 °C for 72 h. Later, they were thoroughly washed with distilled water several times to remove any potassium impurity and then initially air-dried for 48 h followed by drying at 120 °C for 6 h. The dried mass thus obtained was then finely ground to a particle size less than a micron. This material was finally calcined at 500 °C for 6 h. Platinum ($Pt(NH_3)_4(NO_3)_2$, Aldrich) was impregnated over $\gamma$-$Al_2O_3$ (203 $m^2/g$, Sasol), $Ce_{0.2}Zr_{0.8}O_2$ and $Ce_{0.8}Zr_{0.2}O_2$ supports using the incipient wetness method. All catalysts were dried in an oven at 120 °C for 24 h and calcined at 500 °C for 6 h.

The BET specific surface area was measured by nitrogen adsorption at −196 °C using a Micromeritics (ASAP-2400) surface area measurement apparatus. The XRD patterns were recorded using a Rigaku 2155D6 diffractometer (Ni filtered Cu$K_\alpha$ radiation, 40 kV, 50 mA).

$H_2$ pulse chemisorptions were performed in a multifunction apparatus [21]. About 200 mg of catalyst was placed in a quartz reactor. Before pulse chemisorption, the sample was reduced in 5% $H_2$/Ar at 400 °C for 3 h and purged in Ar at the same temperature for 3 h. The catalyst was then cooled to 27 °C in flowing Ar and was kept at this temperature during the entire experiment. Hydrogen pulse chemisorption was started at 27 °C using 5% $H_2$/Ar and repeated at 7 min intervals until the hydrogen peaks on the chromatograph became identical. The catalyst was flushed with pure Ar whereby nonchemisorbed hydrogen desorbed from the sample. Then once again, the catalyst was exposed to 5% $H_2$/Ar. Subtracting the responses from the two experiments gives an area correlating with the amount of chemisorbed $H_2$ on Pt. 5% $H_2$/Ar and Ar (ultra high purity, 99.999%) were used without further purification. The calculation methods of metal dispersion, surface area and average crystallite diameter are the same as those in [22] on assuming the adsorption stoichiometry of one hydrogen atom per Pt surface atom ($H/Pt_s = 1$).

Activity tests were carried out using a fixed-bed quartz reactor (6 mm ID). Before testing the catalysts, they were heated in $N_2$ at 400 °C for 1 h, reduced in 5% $H_2/N_2$ at 400 °C for 1 h, and then cooled down to the reaction temperature. The reaction temperature was changed from 50 to 100 °C to see the activity at low temperatures. The tests were carried out at the GHSV of 18,600 $cm^3/g_{cat}$ h and 1 atm. The catalysts were held in place with glass-wool plugs. 5% CO ($H_2$ balance, ultra high purity) and air were used as reactants. Only stoichiometric amounts of $O_2$ ($CO/O_2 = 2/1$) were employed to investigate the selectivity to $CO_2$ other than $H_2O$. All gases were controlled using mass flow controllers (Brooks). The concentration of CO in the product was measured with an on-line CO analyzer (Thermo-Environmental Instrument, 48C, USA) after removing water using a drierite moisture trap. The concentrations of $O_2$, $CH_4$, and $CO_2$ were measured by a gas chromatograph (HP 6890) with a TCD detector and a Hayesep DB column. The concentrations of $H_2O$ and $H_2$ were only measured approximately by GC. The conversions of CO and $O_2$ and the selectivity of CO were defined as follows:

$$\text{CO conversion } (\%) = [CO_2]_{out}/[CO]_{in} \times 100$$

$$O_2 \text{ conversion } (\%) = [[O_2]_{in} - [O_2]_{out}]/[O_2]_{in} \times 100$$

$$CO_2 \text{ selectivity } (\%) = 0.5[CO_2]_{out}/[[O_2]_{in} - [O_2]_{out}] \times 100.$$

## 3. Results and discussion

### 3.1. Characterization

Figure 1 depicts XRD patterns of $Ce_{0.2}Zr_{0.8}O_2$ and $Ce_{0.8}Zr_{0.2}O_2$ supports prepared by the one-step co-precipitation/digestion after calcination step at 500 °C for 6 h. In the case of $Ce_{0.8}Zr_{0.2}O_2$, typical XRD patterns of the mixed oxides (indexed in the cubic Fm3m space group) can be seen. The patterns consist of

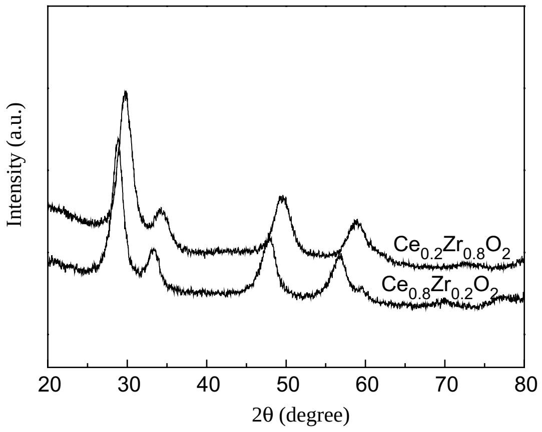

Figure 1. XRD patterns of co-precipitated $Ce_{0.2}Zr_{0.8}O_2$ and $Ce_{0.8}Zr_{0.2}O_2$ supports.

Table 1
Characteristics of $\gamma$-$Al_2O_3$, $Ce_{0.2}Zr_{0.8}O_2$ and $Ce_{0.8}Zr_{0.2}O_2$ supports

| | $\gamma$-$Al_2O_3$ | $Ce_{0.2}Zr_{0.8}O_2$ | $Ce_{0.8}Zr_{0.2}O_2$ |
|---|---|---|---|
| Phase | – | Tetragonal | Cubic |
| BET surface area ($m^2/g$)[a] | 203 | 166 | 174 |
| Crystallite size (nm)[b] | – | 4.6 | 5.4 |

[a] Estimated from $N_2$ adsorption at −196 °C.
[b] Estimated from XRD.

six main reflections, typical of a cubic, fluorite structure of $CeO_2$, corresponding to the (111), (200), (220), (311), (222), and (400) planes. It is generally accepted that $Ce_{1-x}Zr_xO_2$ preferably crystallizes into a cubic structure if $x$ is lower than 0.5 [17]. The presence of only the cubic phase indicates that Ce and Zr are highly homogeneously distributed. On the contrary, $Ce_{0.2}Zr_{0.8}O_2$ shows a tetragonal phase. The evidence of only the tetragonal phase also indicates that Ce and Zr are highly homogeneously distributed. Meeyoo and co-workers [17] obtained clear cubic phase using a sol–gel technique. However, they could not get clear tetragonal phase using the same technique. Thus, it was confirmed that the co-precipitation method employed in this study is effective in achieving both cubic and tetragonal phase of Ce—$ZrO_2$ by controlling Ce/Zr ratios.

Table 1 summarizes characteristics of $\gamma$-$Al_2O_3$, $Ce_{0.2}Zr_{0.8}O_2$ and $Ce_{0.8}Zr_{0.2}O_2$ supports. BET surface area of $\gamma$-$Al_2O_3$ is 203 $m^2/g$. The surface area of $Ce_{0.8}Zr_{0.2}O_2$ is 174 $m^2/g$ and that of $Ce_{0.2}Zr_{0.8}O_2$ is 166 $m^2/g$ after calcination at 500 °C for 6 h. The surface area values are quite high compared with reported data for similar compositions prepared by other chemical routes such as a sol–gel, hydrothermal, microwave hydrothermal, micro-emulsion and high-energy ball milling [17,23,24]. It was reported that $Ce_{0.25}Zr_{0.75}O_2$ and $Ce_{0.75}Zr_{0.25}O_2$ prepared by a sol–gel method had BET surface areas of 120 and 108 $m^2/g$, respectively, after calcination at 500 °C for 4 h [17]. It means that BET surface areas of co-precipitated Ce—$ZrO_2$ materials are about 50 $m^2/g$ higher than those using other methods. Therefore, high surface areas of Ce—$ZrO_2$ prepared by the co-precipitation method are another evidence that the co-precipitation method is more effective than other methods. The particle sizes of $Ce_{0.8}Zr_{0.2}O_2$ and $Ce_{0.2}Zr_{0.8}O_2$ are 5.4 and 4.6 nm, respectively. It indicates that nano-sized particles were successfully achieved by the co-precipitation method.

Table 2 gives the hydrogen uptake amounts and the dispersion values estimated from them for the catalysts containing 1% Pt. The $H_2$ uptake amounts of supports are only negligible (less than 1% of the Pt containing catalysts). The $H_2$ uptake decreases in the order: $Pt/Ce_{0.8}Zr_{0.2}O_2 > Pt/CeO_2 > Pt/Ce_{0.2}Zr_{0.8}O_2 > Pt/ZrO_2 \gg Pt/Al_2O_3$. The estimated dispersion values exceed 100% for all the catalysts except 1% $Pt/Al_2O_3$. This is possibly caused by the hydrogen spill-over to supports [25,26]. Though dispersion values could not be measured quantitatively, it is clear that $Ce_{0.8}Zr_{0.2}O_2$ has enhanced ability of $H_2$ uptake. It is likely that the enhanced $H_2$ uptake of $Ce_{0.8}Zr_{0.2}O_2$ has beneficial effect on CO oxidation (figure 2). However, the $H_2$ uptake of the catalysts does not play a key role in CO oxidation. Even though the $H_2$ uptake value of 1% $Pt/ZrO_2$ is much higher than that of 1% $Pt/Al_2O_3$, the former did not show any activity in CO oxidation.

### 3.2. CO oxidation in excess of $H_2$

Figure 2 shows CO conversion with reaction temperature over 1% Pt catalysts. Among the catalysts tested, 1% $Pt/Ce_{0.8}Zr_{0.2}O_2$ exhibited the highest activity. The CO conversion was maximized at 60 °C with stoichiometric amounts of $O_2$. The decrease in CO conversion at high temperature was caused by hydrogen oxidation. $H_2O$ peaks without other peaks such as $CH_4$ were observed in GC results. In the case of 1% $Pt/Ce_{0.2}Zr_{0.8}O_2$, the CO conversion increased with reaction temperature. However, the activity was much lower than that of 1% $Pt/Ce_{0.8}Zr_{0.2}O_2$. The CO conversion of 1% $Pt/CeO_2$ was maximized at 60 °C like that of 1% $Pt/Ce_{0.8}Zr_{0.2}O_2$. However, the activity was about half of the activity of the latter. 1% $Pt/ZO_2$ showed only negligible activity. The CO conversion of 1% $Pt/Al_2O_3$ was about 1% within the temperature range. Therefore, it was confirmed that 1% Pt supported on cubic $Ce_{0.8}Zr_{0.2}O_2$ has remarkable activity in CO oxidation using stoichiometric amounts of $O_2$ in excess $H_2$ at low temperatures. It should be noted that active CO oxidation catalyst at low temperatures (<100 °C) is very rare in the presence of excess $H_2$. It was reported that 5% $Pt/\gamma$-$Al_2O_3$ showed 23% CO conversion at 100 °C, 52% at 150 °C, and 54% at 200 °C using stoichiometric amounts of $O_2$ [6]. Even though 1% $Pt/Ce_{0.8}Zr_{0.2}O_2$ has 5 times less Pt content, it exhibited much higher activity even at 60 °C.

According to the BET surface area results, $\gamma$-$Al_2O_3$ shows the highest surface area (203 $m^2/g$). $Ce_{0.2}Zr_{0.8}O_2$

Table 2
$H_2$ chemisorption data on 1% Pt catalysts

| Catalyst | $Ce_{0.8}Zr_{0.2}O_2$ | $Ce_{0.2}Zr_{0.8}O_2$ | $CeO_2$ | $ZrO_2$ | $\gamma$-$Al_2O_3$ |
|---|---|---|---|---|---|
| $H_2$ uptake ($\mu$mol/g) | 35.9 | 30.7 | 34.3 | 27.1 | 15.0 |
| Dispersion (%) | 140.0 | 120.0 | 133.8 | 105.9 | 58.4 |

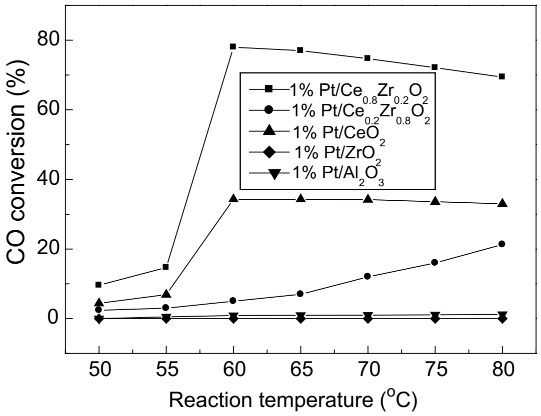

Figure 2. CO conversion with reaction temperature over 1% Pt catalysts (reaction conditions: $CO/O_2$ = 2/1, GHSV = 16,800 mL/h $g_{cat}$).

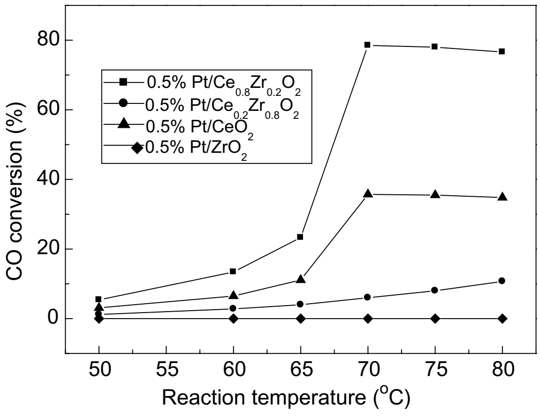

Figure 3. CO conversion with reaction temperature over 0.5% Pt catalysts (reaction conditions: $CO/O_2 = 2/1$, GHSV = 16,800 mL/h $g_{cat}$).

and $Ce_{0.8}Zr_{0.2}O_2$ show 166 and 174 $m^2/g$, respectively. Consequently, it is concluded that the effect of surface area on CO oxidation activity is not pronounced. On the contrary, it can be speculated that nano-sized $Ce—ZrO_2$ particles (4–5 nm) play significant role in good activity resulting from fine-dispersion of Pt on $Ce—ZrO_2$ supports. The fact that 1% $Pt/ZrO_2$ showed only negligible activity indicates that Ce is the most important component to achieve high activity in CO oxidation in low temperatures. Improved CO conversions at low temperatures using stoichiometric amounts of $O_2$ were also reported for Ce-promoted $Pt/\gamma$-$Al_2O_3$ [6]. It was found that $CeO_2$ promotes CO oxidation by using lattice oxygen, improving oxygen supply to Pt on $CeO_2$ in low-oxygen-concentration environment [15]. It was also reported that the cubic phase of $Ce—ZrO_2$ has more OSC and is more easily reducible than the tetragonal phase [17,19,20]. As a result, it was found that cubic $Ce_{1-x}—Zr_xO_2$ ($x < 0.5$) showed better CO oxidation performance than tetragonal $Ce_{1-x}—Zr_xO_2$ ($x > 0.5$) [17]. Therefore, high activity of $Pt/Ce_{0.8}Zr_{0.2}O_2$ can be interpreted as the high OSC and nano-sized nature of cubic $Ce_{0.8}Zr_{0.2}O_2$.

Figure 3 illustrates CO conversion with reaction temperature over 0.5% Pt catalysts. 0.5% $Pt/Ce_{0.8}Zr_{0.2}O_2$ also exhibited the highest activity among the catalysts tested. The maximum CO conversion (79%) was obtained at 70 °C. The CO conversion of 0.5% $Pt/Ce_{0.2}Zr_{0.8}O_2$ increased with reaction temperature. But the activity was much lower than that of 0.5% $Pt/Ce_{0.8}Zr_{0.2}O_2$, which was similar to the results of 1% Pt catalysts. The CO conversion of 0.5% $Pt/CeO_2$ was maximized at 70 °C like that of 0.5% $Pt/Ce_{0.8}Zr_{0.2}O_2$. However, the activity was about half of the activity of the latter. 0.5% $Pt/ZO_2$ did not show any activity within the temperature range tested. Consequently, it was confirmed that 0.5% Pt supported on cubic $Ce_{0.8}Zr_{0.2}O_2$ has remarkable activity in CO oxidation in excess $H_2$ at low temperatures.

$CO_2$ selectivity is one of the important factors in CO oxidation in the presence of excess $H_2$, because $H_2$ oxidation into $H_2O$ will decrease the efficiency of the system. Therefore, $O_2$ should react with CO other than $H_2$. To avoid $H_2$ loss, we used stoichiometric amounts of $O_2$ in CO oxidation. $CO_2$ selectivity with reaction temperature over Pt catalysts is shown in figure 4. Both 0.5% and 1% $Pt/Ce_{0.2}Zr_{0.8}O_2$ catalysts showed 100% $CO_2$ selectivity, indicating that $O_2$ selectively oxidized CO into $CO_2$ without oxidation of $H_2$. 0.5% $Pt/Ce_{0.8}Zr_{0.2}O_2$ exhibited good $CO_2$ selectivity. $CO_2$ selectivity was 100% from 50 to 60 °C and 92% at 80 °C. 1% $Pt/Ce_{0.8}Zr_{0.2}O_2$ showed 96% selectivity at 60 °C, 90% at 70 °C and 85% at 80 °C. It means that $H_2O$ formation from $H_2$ oxidation occurred at relatively high temperature.

To see the stability of 1% $Pt/Ce_{0.8}Zr_{0.2}O_2$, long-run test was conducted for 50 h. The results are shown in figure 5. About 78% CO conversion was steadily obtained during the test. The $CO_2$ selectivity of 96%

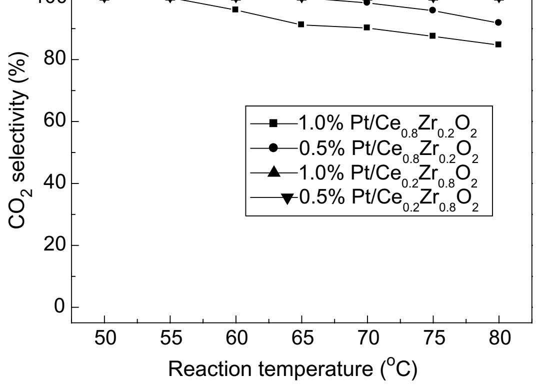

Figure 4. $CO_2$ selectivity with reaction temperature over Pt catalysts (reaction conditions: $CO/O_2 = 2/1$, GHSV = 16,800 mL/h $g_{cat}$).

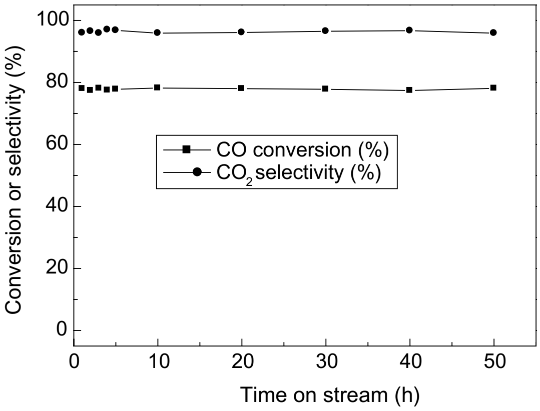

Figure 5. Stability test over 1% Pt/$Ce_{0.8}Zr_{0.2}O_2$ catalyst (reaction conditions: $T = 60$ °C, $CO/O_2 = 2/1$, GHSV = 16,800 mL/h $g_{cat}$).

was also maintained for 50 h. It indicates that 1% Pt/$Ce_{0.8}Zr_{0.2}O_2$ is very stable in CO oxidation at low temperatures.

In summary, Pt/$Ce_{0.8}Zr_{0.2}O_2$ catalyst exhibited high CO conversion (about 78%) and high $CO_2$ selectivity (about 96%) at low temperatures (60–70 °C). Increasing the temperature did not enhance the CO conversion but decreased the selectivity to $CO_2$ owing to the competing $H_2$ oxidation. It was found that cubic Ce—$ZrO_2$ support is more effective than tetragonal support due to higher OSC.

## 4. Conclusions

The catalysts, Pt/$Ce_{0.8}Zr_{0.2}O_2$ (Pt content = 1% and 0.5%) exhibited remarkably high CO conversion at low temperatures (60–70 °C) using stoichiometric amounts of $O_2$ in the preferential CO oxidation. Moreover, the catalytic activity was very stable for 50 h at 60 °C. Ceria addition in $ZrO_2$ support leads to significant improvement in the activity. The benefit of cubic $Ce_{0.8}Zr_{0.2}O_2$ support is probably due to high OSC. Co-precipitation method was found to be very effective to prepare high surface area and nano-crystalline nature of both cubic and tetragonal Ce—$ZrO_2$.

## References

[1] A.F. Ghenciu, Curr. Opin. Solid State Mater. Sci. 6 (2002) 389.
[2] P.G. Gray and M.I. Petch, Platinum Metals Rev. 44 (2000) 108.
[3] S. Golunski, Platinum Metals Rev. 42 (1998) 2.
[4] P.G. Gray and J.C. Frost, Energy Fuels 12 (1998) 1121.
[5] A. Docter and A. Lamm, J. Power Sources 84 (1999) 194.
[6] I.H. Son and A.M. Lane, Catal. Lett. 76 (2001) 151.
[7] G.B. Hoflund and W.S. Epling, Recent Res. Devel. Catal. 1 (1996) 31.
[8] H. Igarashi, H. Uchida, M. Suzuki, Y. Sasaki and M. Watanabe, Appl. Catal. 159 (1997) 159.
[9] S.H. Oh and R.M. Sinkevitch, J. Catal. 142 (1993) 254.
[10] M. Watanabe, H. Uchida, H. Igarashi and M. Suzuki, Chem. Lett. (1995) 21.
[11] M.J. Kahlich, H.A. Gasteiger and R.J. Behm, J. Catal. 171 (1997) 93.
[12] G.K. Bethke and H.H. Kung, Appl. Catal. A 194–195 (2000) 43.
[13] A. Trovarelli, C. de Leitenburg, M. Boaro and G. Dolcetti, Catal. Today 50 (2000) 353.
[14] A. Trovarelli, Catal. Rev. – Sci. Eng. 38 (1996) 439.
[15] J. Kaspar, P. Fornasiero and M. Graziani, Catal. Today 50 (1999) 285.
[16] S. Rossignol, F. Gerard and D. Duprez, J. Mater. Chem. 9 (1999) 1615.
[17] M. Thammachart, V. Meeyoo, T. Risksomboon and S. Osuwan, Catal. Today 68 (2001) 53.
[18] C. Bozo, N. Guilhaume, E. Garbowski and M. Primet, Catal. Today 594 (2000) 33.
[19] S. Wang and G.Q. Lu, Appl. Catal. A 169 (1998) 271.
[20] S. Rossignol, Y. Madier and D. Duprez, Catal. Today 509 (1999) 261.
[21] H.S. Potdar, H.-S. Roh, K.-W. Jun, M. Ji and Z.-W. Liu, Catal. Lett. 84 (2002) 95.
[22] J.R. Anderson and K.C. Pratt, in: *Introduction to Characterization and Testing of Catalysts*, Vol. 1 (Academic Press, Australia, 1985).
[23] S.M. Stagg-Williams, F.B. Noronha, G. Fendley and D.E. Resasco, J. Catal. 194 (2000) 240.
[24] H.S. Potdar, S.B. Deshpande, A.S. Deshpande, S.P. Gokhale, Y.B. Khollam, A.J. Patil and S.K. Date, Mater. Chem. Phys. 74 (2001) 306.
[25] C. Dall'Agnol, A. Gervasini, F. Morazzoni, F. Pinna, G. Strukul and L. Zanderighi, J. Catal. 96 (1985) 106.
[26] W.K. Jozwiak, React. Kinet. Catal. Lett. 30 (1986) 345.